S04

Proceedings of the 5th International Conference on Inverse Problems in Engineering: Theory and Practice, Cambridge, UK, 11-15 July 2005

A COMPARISON OF TWO DIFFERENT APPROACHES FOR THE DAMAGE IDENTIFICATION PROBLEM

E.H. SHIGUEMORI[1], L.D. CHIWIACOWSKY[1], H.F. de CAMPOS VELHO[1], P. GASBARRI[2] and J.D.S. SILVA[1]
[1]*Laboratório Associado de Computação e Matemática Aplicada (LAC), Instituto Nacional de Pesquisas Espaciais (INPE), Caixa Postal 515, 12245-970, São José dos Campos, SP, Brazil*
e-mail: [elcio, leodc, haroldo, demisio]@lac.inpe.br
[2]*Dipartimento di Ingegneria Aerospaziale e Astronautica, Università degli Studi di Roma "La Sapienza", Rome, Italy*
e-mail: paolo.gasbarri@uniroma1.it

Abstract - This work deals with structural damage detection using synthetic displacement measurements as experimental data to be used by two different methodologies: the conjugate gradient method with the adjoint equation and an artificial neural network. Both techniques have been employed in order to place and quantify the time-variable damage in a simple truss structure. Estimation errors have been reported in order to make possible a comparison of the two methodologies.

1. INTRODUCTION

Considerable research and effort over the last few decades has taken place in the field of system identification problem, for different reasons. One of the most interesting applications involves the monitoring of structural integrity through the identification of damage. It is well known that damage modifies the dynamic response of a structure and, at the same time, that changes in its behavior may be associated with the decay of the system's mechanical properties [16].

The damage identification problem is displayed as an inverse vibration problem, since the damage evaluation is achieved through the determination of the stiffness coefficient variation, or the stiffness coefficient by itself. The inverse problem solution is generally unstable, therefore, small perturbations in the input data, like random errors inherent to the measurements used in the analysis, can cause large oscillations on the solution. In general the inverse problem, i.e. the ill-posed problem, is presented as a well-posed functional form, whose solution is obtained through an optimization procedure.

Based on these considerations, several works have examined the use of measured variations in dynamic behavior to detect structural damage. A variety of experimental, numerical and analytical techniques has already been proposed to solve the damage identification problem, and have received notable attention due to its practical applications [7]. These methods are usually classified under several categories, such as frequency and time domain methods, parametric and non-parametric models, deterministic and stochastic approaches [6, 4].

Among the classical methods, recently the use of the conjugate gradient method with the adjoint equation [1, 12], or Variational Approach, which has been used successfully in thermal sciences [6], has also been presented as a satisfactory choice to face the damage identification problem.

Some works regarding the use of the variational approach in inverse vibration problems can be found in the literature, for instance, Huang [10, 11] has estimated the time-dependent stiffness coefficients considering spring-mass systems with one and multiple degrees of freedom. Also, Castello and Rochinha [5] have identified the elastic and damping parameters of a bar-like structure using the adjoint equation approach. On the other hand, among the non-classical stochastic methods, the Artificial Neural Networks (ANNs) represent a powerful choice for solving non trivial problems. The fault tolerance, generalization capabilities of ANN's make them attractive to approach inverse problems.

Works regarding the use of ANN methods to solve the damage identification problem have been reported in the literature employing different neural network models, either multi-layer perceptrons [17, 3, 18] or radial basis functions [2, 13]. In this work both the Variational approach and ANN method have been used to estimate the time-dependent stiffness of a simple truss structure. The estimation errors concerning both methodologies have been employed in order to evaluate the estimation quality of the two different techniques.

2. THE DIRECT PROBLEM

The N-DOF damped system considered in this work is presented in Figure 1 and the mathematical formulation of this forced vibration systems is given by

$$\mathbf{M}\,\ddot{\mathbf{x}}(t) + \mathbf{C}\,\dot{\mathbf{x}}(t) + \mathbf{K}(t)\,\mathbf{x}(t) = \mathbf{f}(t)\,, \tag{1}$$

with initial conditions

$$\mathbf{x}(0) = \mathbf{x}_0 \quad \text{and} \quad \dot{\mathbf{x}}(0) = \dot{\mathbf{x}}_0 \,. \tag{2}$$

In eqn. (1) $\mathbf{M}$ represents the system mass matrix, $\mathbf{K}(t)$ the time-dependent stiffness matrix, $\mathbf{C}$ the damping matrix, $\mathbf{f}(t)$ the external forces vector, and $\mathbf{x}(t)$ the displacements vector. There exists no analytical solution for eqns. (1)-(2) for any arbitrary functions of $\mathbf{K}(t)$, $\mathbf{C}$, and $\mathbf{f}(t)$. For this reason the numerical solution with the *Newmark* method [15] is applied to solve the direct problem. This problem calculates the system displacement vector $\mathbf{x}(t)$, if initial conditions, system parameters $\mathbf{M}$, $\mathbf{K}(t)$ and $\mathbf{C}$, and the time-dependent external forces $\mathbf{f}(t)$ are known.

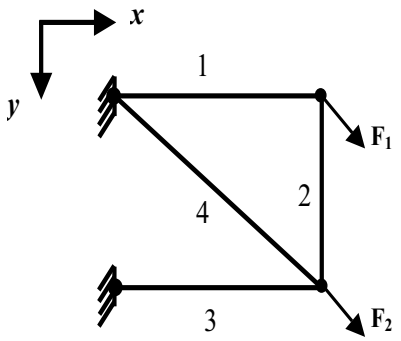

Figure 1: The truss structure considered in this work.

3. THE VARIATIONAL APPROACH

The goal of this work is to recover the unknown time-dependent stiffness coefficients from the synthetic system displacement measurements of a truss structure with N-DOF (Figure 1). The inverse analysis with the conjugate gradient method involves the following steps [1, 12]: (i) the solution of the direct problem; (ii) the solution of the sensitivity problem; (iii) the solution of the adjoint problem and the gradient equation; (iv) the conjugate gradient method of minimization; (v) the stopping criteria. Next, a brief description of basic procedures involved in each of these steps is presented.

3.1. The Sensitivity Problem

This problem involves N unknown time-dependent stiffness parameters, which constitute the elements of the stiffness matrix $\mathbf{K}(t) = f[\boldsymbol{\mathcal{K}}(t)]$, where $\boldsymbol{\mathcal{K}}(t) = [K_1(t), ..., K_N(t)]$ and the parameters $K_i(t)$, $i = 1, ..., N$ represent the structural stiffness parameters of the finite element; for instance for a bar-like structure $K_i = EA/L_e$, where E is the Young's module, A is the cross section area and L_e is the length of the finite element. In order to derive the sensitivity problem for each unknown function $K_i(t)$, each unknown stiffness parameter should be perturbed at a time. Supposing that $K_i(t)$ is perturbed by a small amount $\triangle K_i(t)\,\delta(i-j)$, where the $\delta(\cdot)$ is the Dirac-delta function and $j = 1, \ldots, N$, results in a small change in displacements by the amounts of $\triangle x_{ij}(t)$. The sensitivity problem is obtained by replacing in the direct problem, Eqs. (1)-(2), $K_i(t)$ by $K_i(t) + \triangle K_i(t)\,\delta(i-j)$, $x_i(t)$ by $x_i(t) + \triangle x_{ij}(t)$, and by subtracting the original direct problem from the resulting expression, and also by neglecting the second-order terms. Therefore, N sensitivity problems have been obtained, since $j = 1, \ldots, N$, i.e., a different sensitivity problem for each perturbed stiffness parameter. The sensitivity problem is defined by the following system of differential equations

$$\mathbf{M}\,\triangle\ddot{\mathbf{x}}_j(t) + \mathbf{C}(t)\,\triangle\dot{\mathbf{x}}_j(t) + \mathbf{K}(t)\,\triangle\mathbf{x}_j(t) = \triangle\mathbf{K}_j(t)\,\mathbf{x}(t)\,, \tag{3}$$

where $j = 1, \ldots, N$ and with initial conditions

$$\triangle\mathbf{x}_j(0) = 0 \quad \text{and} \quad \triangle\dot{\mathbf{x}}_j(0) = 0\,. \tag{4}$$

3.2. The Adjoint Problem and the Gradient Equation

The inverse problem is to be solved as an optimization problem requiring that the unknown function $\boldsymbol{\mathcal{K}}(t)$ minimize the functional $J[\boldsymbol{\mathcal{K}}(t)]$ defined by

$$\boldsymbol{J}[\boldsymbol{\mathcal{K}}(t)] = \int_0^{t_f} [\,\mathbf{x}(t) - \mathbf{x}^{exp}(t)]^{\mathrm{T}}\,[\,\mathbf{x}(t) - \mathbf{x}^{exp}(t)]\;\, dt, \tag{5}$$

where t_f is the final time, $\mathbf{x}(t)$ and $\mathbf{x}^{exp}(t)$ are the computed and measured displacements at time t, respectively. For solving the minimization problem (5), the *Lagrange* multiplier vector $\boldsymbol{\lambda}(t)$ is usually used to associate the constraints (1) to the functional form

$$\boldsymbol{J}[\boldsymbol{\mathcal{K}}] = \int_0^{t_f} \left[\mathbf{x} - \mathbf{x}^{exp}\right]^{\mathrm{T}} \left[\mathbf{x} - \mathbf{x}^{exp}\right] \, dt + \int_0^{t_f} \boldsymbol{\lambda}^{\mathrm{T}} \left\{\mathbf{M}\,\ddot{\mathbf{x}} + \mathbf{C}\,\dot{\mathbf{x}} + \mathbf{K}\,\mathbf{x} - \mathbf{f}\right\} \, dt\,. \tag{6}$$

Computing the differential of the functional form and knowing that the coefficient of $\triangle x$ shall vanish, for convenience the vector $\boldsymbol{\lambda}$ has been chosen to be the solution of the adjoint problem:

$$\mathbf{M}\,\ddot{\boldsymbol{\lambda}}(t) - \mathbf{C}(t)\,\dot{\boldsymbol{\lambda}}(t) + \mathbf{K}(t)\,\boldsymbol{\lambda}(t) = 2\left[\mathbf{x}^{exp}(t) - \mathbf{x}(t)\right]\,, \tag{7}$$

with final conditions

$$\boldsymbol{\lambda}(t_f) = 0 \quad \text{and} \quad \dot{\boldsymbol{\lambda}}(t_f) = 0\,. \tag{8}$$

Applying the variational theory [12], the left term is employed to determine the gradient $\boldsymbol{J}[\boldsymbol{\mathcal{K}}]$, which is given by

$$\boldsymbol{J}'_j[\boldsymbol{\mathcal{K}}] = \int_0^{t_f} \boldsymbol{\lambda}^{\mathrm{T}} \triangle\tilde{\mathbf{K}}_j\,\mathbf{x}\,dt\,, \tag{9}$$

where $\triangle\tilde{\mathbf{K}}_j$ refers to the j^{th} perturbed stiffness matrix, i.e. $\triangle\tilde{\mathbf{K}}_j = \partial[\triangle\mathbf{K}]/\partial K_j(t)$.

3.3. The Conjugate Gradient Method of Minimization

The iterative procedure based on the conjugate gradient method is used for the estimation of the unknown stiffness parameters $\boldsymbol{\mathcal{K}}$ given in the form [1, 12]:

$$\boldsymbol{\mathcal{K}}^{n+1} = \boldsymbol{\mathcal{K}}^n - \boldsymbol{\beta}^n\,\mathbf{P}^n, \quad n = 0, 1, 2, ...,$$

$$\mathbf{P}^n = \boldsymbol{J}'^{\,n} + \boldsymbol{\gamma}^n\,\mathbf{P}^{n-1}, \quad \text{with} \quad \boldsymbol{\gamma}^0 = 0, \tag{10}$$

where $\boldsymbol{\beta}^n$ is the step size vector, $\mathbf{P}^n$ is the direction of descent vector and $\boldsymbol{\gamma}^n$ is the conjugate coefficient vector. The step size vector $\boldsymbol{\beta}^n$, appearing in eqn. (10), is determined by minimizing the functional vector $\boldsymbol{J}[\boldsymbol{\mathcal{K}}^{n+1}]$ given by eqn. (5) with respect to $\boldsymbol{\beta}^n$. For the stopping criterion the discrepancy principle has been taken as

$$J[\boldsymbol{\mathcal{K}}^{n+1}] < \epsilon^2, \tag{11}$$

where $\epsilon^2 = N\sigma^2 t_f$, and σ is the standard deviation of the measurements errors.

4. MULTILAYER PERCEPTRON NEURAL NETWORK

Artificial Neural Networks (ANN) have become important tools for information processing [9]. Much research has been conducted in pursuing new neural network models and adapting the existing ones to solve real life problems, such as those in engineering [9]. ANNs are made of arrangements of processing elements called neurons. The artificial neuron model basically consists of a linear combiner followed by an activation function (Figure 2(a)), given by:

$$y_k = \varphi\left(\sum_{j=1}^{n} w_{kj}\,x_j + b_k\right)\,, \tag{12}$$

where w_{kj} are the connections weights, b_k is a threshold parameter, x_j is the input vector and y_k is the output of the k^{th} neuron.

Arrangements of such units form the ANNs that are characterized by:

- Very simple neuron-like processing elements;
- Weighted connections between the processing elements;
- Highly parallel processing and distributed control;
- Automatic learning of internal representations.

ANNs aim to explore the massively parallel network of simple elements in order to yield a result in a very short time slice and, at the same time, with insensitivity to loss and failure of some of the elements of the network. These properties make artificial neural networks appropriate for application in pattern recognition, signal processing, image processing, financing, computer vision, engineering, etc.

There exist different ANN architectures that are dependent upon the learning strategy adopted. This paper briefly describes the Multilayer Perceptron (MLP) with error backpropagation learning. Detailed introductions on ANNs can be found in [9] and [14]. MLP with backpropagation learning algorithm, are feedforward networks composed of an input layer, an output layer, and a number of hidden layers, whose aim is to extract high order statistics from the input data [8]. Figure 2(b) depicts a multilayer neural network with a hidden layer.

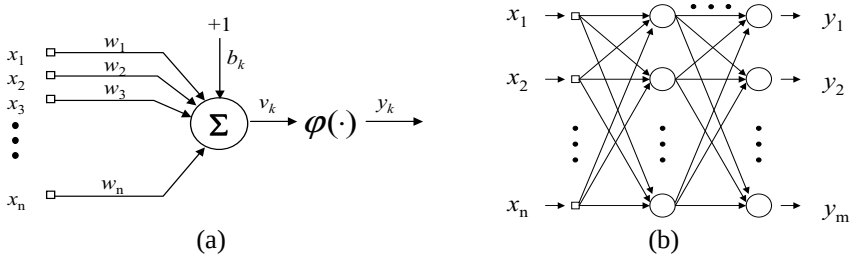

(a) (b)

Figure 2: (a) Single Neuron, (b) Multilayer Neural Network.

Functions $\varphi(\cdot)$ provide the activation for the neuron. Neural networks will solve nonlinear problems, if non-linear activation functions are used for the hidden and/or the output layers. From several activation functions, the sigmoid are commonly used:

$$\text{logistic function :} \qquad \varphi(v) = \frac{1}{1+\exp(-av)}\,;$$

$$\text{bipolar function :} \qquad \varphi(v) = \frac{1-\exp(-av)}{1+\exp(-av)}\,. \tag{13}$$

A feedforward network can transform input vectors of real values onto output vector of real values. The connections among the several neurons (Figure 2) have associated weights that are adjusted during the learning process, thus changing the performance of the network. Two distinct phases can be devised while using an ANN: the training phase (learning process) and the run phase (activation of the network). The training phase consists of adjusting the weights for the best performance of the network in establishing the mapping of many input/output vector pairs. Once trained, the weights are fixed and the network can be presented to new inputs for which it calculates the corresponding outputs, based on what it has learned.

The error backpropagation training is a supervised learning algorithm that requires both input and output (desired) data. Such pairs permit the calculation of the error of the network as the difference between the calculated output and the desired vector. The weight adjustments are conducted by backpropagation such error to the network, governed by a change rule. The weights are changed by an amount proportional to the error at that unit, times the output of the unit feeding the weight. Equation (14) shows the general weight correction according to the so-called delta rule

$$\Delta w_{kj} = \eta\, \delta_k\, y_j\,, \tag{14}$$

where, δ_k is the local gradient, y_j is the input signal of neuron k, and η is the learning rate parameter that controls the strength of change.

5. INVERSE PROBLEM SOLUTION BY ANN

In this work a MLP Neural Network is employed to solve the problem of the estimation of the time-dependent stiffness coefficients of a truss structure (see Figure 1). This truss structure is composed by 4 bars and clamped at one end. The unknown transient stiffness coefficients have been assumed as:

$$\boldsymbol{\mathcal{K}}_1(t) = a_1\left(\frac{E\,A}{L_1}\right) - b_1\left(\frac{E\,A}{L_1}\right)\sin\left(c_1\frac{2\pi\,t}{t_f}\right); \qquad \boldsymbol{\mathcal{K}}_2(t) = a_2\left(\frac{E\,A}{L_2}\right) + b_2\left(\frac{E\,A}{L_2}\right)\cos\left(c_2\frac{2\pi\,t}{t_f}\right);$$

$$\boldsymbol{\mathcal{K}}_3(t) = a_3\left(\frac{E\,A}{L_3}\right) + b_3\left(\frac{E\,A}{L_3}\right)\cos\left(c_3\frac{2\pi\,t}{t_f}\right); \qquad \boldsymbol{\mathcal{K}}_4(t) = a_4\left(\frac{E\,A}{L_4}\right) + b_4\left(\frac{E\,A}{L_4}\right)\sin\left(c_4\frac{2\pi\,t}{t_f}\right). \tag{15}$$

In order to give a good information to the neural network, a history of 15 time steps is used, resulting in 60 inputs and 4 desired output units. For this reason, stiffness coefficients have been estimated from the fifteenth time step. Although different neural networks topologies have been used, varying the number of hidden layers and the number of neurons in each layer, one hidden layer with 10 neurons was sufficient to obtain good results. The sigmoid activation function has been used in both hidden and output layers. Besides that, some numerical experiments have been developed using a different model of neural network, the Radial Basis Function (RBF). The estimation results obtained with the RBF model were worst than the ones obtained with the MLP and for this reason they are not presented in this work.

5.1. Training

The training set is built up from the solution of the direct model (eqns. (1) and (2)) assuming several different variations of the stiffness functions (eqns. (15)), generating the respective displacements. For the training phase the desired output of the ANN are the stiffness coefficients, while the input of the ANN are the corresponding measured displacements. For each assumed stiffness coefficient function the corresponding displacement is computed to adjust the weight and bias which will be used in the activation phase. The training set was composed of 32 different functions for the stiffness coefficients. This functions are defined trough the equations (15) where different values for the parameters a_i, b_i and c_i, for $i = 1, \ldots, 4$, have been assumed.

6. NUMERICAL RESULTS

In this work the unknown time-dependent stiffness coefficients are estimated employing two different methodologies: a deterministic one represented by the variational approach, and a stochastic one represented by the artificial neural networks. The estimation results are employed to produce both qualitative and quantitative comparison considering a 4-bar truss structure, clamped at one (see Figure 1).

The referred truss structure is composed by aluminum bars ($\rho = 2700\ kg/m^3$ and $E = 70\ GPa$) with a square cross section area $A = 25.0 \times 10^{-4}\ m^2$, where the nondiagonal elements are $1.0\ m$ long. This numerical example has used the finite element method to calculate the mass and the stiffness matrices that appear in eqn. (1); note that for this example one finite element for each bar has been used. As far as the damping matrix is concerned, it has been assumed that it is proportional to the undamaged stiffness matrix $\mathbf{C} = 5.0 \times 10^{-5}\,\mathbf{K}$. Furthermore, it has been assumed an external force of intensity $\mathbf{f}(t) = 1000.0$ N applied at the vibrating nodes in the positive diagonal direction constant with time and the following initial conditions have been adopted $\mathbf{x}(0) = 0$ and $\dot{\mathbf{x}}(0) = 0$. Numerical simulations have been performed assuming the final time as $t_f = 5.0 \times 10^{-2}$ s and a time step $\triangle t = 5.0 \times 10^{-4}$ s.

The experimental data, i.e the displacements of the nodes of the structure along x and y directions, have been simulated by adding a random perturbation to the exact solution of the direct problem, such that

$$x^{exp}(t) = x(t)\,[1 + \sigma\,\mathcal{R}]\,, \tag{16}$$

where σ is the standard deviation of the noise and $\mathcal{R}$ is a random variable taken from a Gaussian distribution, with zero mean and unit variance. For numerical purposes, the estimation results have been obtained considering two different cases: noiseless ($\sigma = 0$) and noisy experimental data ($\sigma = 1\%$).

In order to evaluate the accuracy of the adopted methodologies, the error between the estimated stiffness coefficients ($\hat{\mathcal{K}}$) and the corresponding exact values ($\mathcal{K}_{exact}$) is defined by

$$E(\hat{\mathcal{K}}) = \left\| \frac{\mathcal{K}_{exact}(t) - \hat{\mathcal{K}}(t)}{\mathcal{K}_{exact}(t)} \right\|_2^2 , \tag{17}$$

where $\|\cdot\|_2$ is the 2-norm. Also, the average error is computed considering the recovered functions for each stiffness coefficient, where M represents the number of functions to be evaluated:

$$\overline{E(\hat{\boldsymbol{\mathcal{K}}}_j)} = E(\hat{\boldsymbol{\mathcal{K}}}_j)_{mean} = \frac{1}{M}\sum_{i=1}^{M} E(\hat{\boldsymbol{\mathcal{K}}}_j)_i\,, \quad \text{where} \quad j = 1, \ldots, 4\,. \tag{18}$$

The standard deviation of the estimation errors for the recovered stiffness coefficients has been calculated using the expression

$$E(\hat{\boldsymbol{\mathcal{K}}}_j)_{std} = \sqrt{\frac{1}{M}\sum_{i=1}^{M}\left(E(\hat{\boldsymbol{\mathcal{K}}}_j)_i - \overline{E(\hat{\boldsymbol{\mathcal{K}}}_j)}\,\right)^2}, \quad \text{where} \quad j = 1, \ldots, 4\,. \tag{19}$$

Table 1 presents the parameters a_i, b_i and c_i ($i = 1, \ldots, 4$) which define, through the equations in (15), the 10 functions to be evaluated.

Table 1: Parameters used in the generalization functions.

Function Case	a_1	a_2	a_3	a_4	b_1	b_2	b_3	b_4	c_1	c_2	c_3	c_4
1	0.9	0.9	0.8	0.9	0.05	0.03	0.07	0.07	2.5	2.0	1.0	1.5
2	0.75	0.75	0.8	0.9	0.05	0.03	0.02	0.07	2.5	2.0	1.0	2.0
3	0.9	0.75	0.9	0.9	0.05	0.03	0.03	0.03	1.5	1.0	1.0	1.5
4	0.9	0.9	0.8	0.9	0.05	0.05	0.05	0.07	2.5	1.0	1.0	1.5
5	0.75	0.75	0.75	0.9	0.05	0.03	0.03	0.01	2.5	2.0	1.0	1.0
6	0.9	0.75	0.8	0.95	0.05	0.03	0.03	0.02	2.5	2.0	1.0	4.0
7	0.9	0.75	0.8	0.9	0.05	0.03	0.03	0.02	2.0	2.0	2.0	1.5
8	0.9	0.75	0.8	0.9	0.01	0.03	0.03	0.07	1.5	1.0	1.5	2.5
9	0.9	0.75	0.8	0.9	0.05	0.03	0.03	0.07	2.5	2.0	1.0	1.5
10	0.75	0.95	0.8	0.9	0.05	0.02	0.03	0.07	2.5	2.0	1.0	1.5

In order to obtain a better comparison between the methodologies, the estimation of the stiffness coefficients for each test function presented in Table 1 has been computed using 50 realizations for different experimental noisy data. Employing these estimation results, average errors and standard deviation of these errors are computed. Statistical information are shown in tables of next Sections, where error $E(.)_{mean}$ is given by eqn. (18). The average of estimations of function type 9 (see Table 1) – average stiffness – is depicted graphically in Sections 6.1 and 6.2, using 50 different experimental noisy data, for both methods (the variational approach and the neural network).

6.1. Variational Approach Results

The variational approach is an iterative procedure based on the conjugate gradient method for which the undamaged configuration has been adopted as the initial guess. It should be noticed that the computed solutions for $\boldsymbol{\mathcal{K}}$, near the initial and final times, are deviated from its correct values because the gradient $\boldsymbol{J}'[\mathbf{K}]$ vanishes for $t = 0$ and $t = t_f$ since $\mathbf{x}(0) = 0$ and $\boldsymbol{\lambda}(t_f) = 0$. For this reason both the first and last time steps have been neglected.

Table 2: Variational Approach - Individual Average Error for noisy data.

Function Case	$E(\hat{\mathcal{K}}_1)_{mean}$	$E(\hat{\mathcal{K}}_2)_{mean}$	$E(\hat{\mathcal{K}}_3)_{mean}$	$E(\hat{\mathcal{K}}_4)_{mean}$
1	0.0066	0.1768	0.0684	0.0007
2	0.0352	0.1430	0.0389	0.0019
3	0.0080	0.1644	0.0976	0.0008
4	0.0062	0.1826	0.0569	0.0006
5	0.0326	0.1624	0.0248	0.0024
6	0.0062	0.1278	0.0451	0.0006
7	0.0084	0.1685	0.0406	0.0009
8	0.0342	0.1221	0.0437	0.0012
9	0.0184	0.1101	0.0480	0.0008
10	0.0084	0.1730	0.0492	0.0010

Tables 2 and 3 present the average error, defined by eqn. (18), and the standard deviation of the error, defined by eqn. (19), respectively. Error values are small ($\boldsymbol{\mathcal{K}}_2 \sim O(10^{-1})$ and the others $\boldsymbol{\mathcal{K}}_i \sim O(10^{-2})$), denoting a good performance of the method for all cases studied. It can be noted that the error for the same stiffness coefficient has the same magnitude for each case. Small values found for the standard deviation imply that the estimation will be a good one, because the errors are systematically small.

Figures 3 and 4 present a qualitative comparison between the estimated stiffness coefficients when noiseless and noisy experimental data are used, respectively, by using the variational approach. In the noiseless case, a perfect reconstruction is performed. However, the method shows its sensibility related to noise, where some oscillations appear in the inverse solution, particularly it is pointed out in the first moments for the $\boldsymbol{\mathcal{K}}_1$.

Table 3: Variational Approach - Individual Standard Deviation for noisy data.

Function Case	$E(\hat{\mathcal{K}}_1)_{mean}$	$E(\hat{\mathcal{K}}_2)_{mean}$	$E(\hat{\mathcal{K}}_3)_{mean}$	$E(\hat{\mathcal{K}}_4)_{mean}$
1	0.0016	0.0623	0.0184	0.0002
2	0.0344	0.0274	0.0101	0.0004
3	0.0028	0.0393	0.0250	0.0002
4	0.0015	0.0546	0.0130	0.0002
5	0.0047	0.0329	0.0044	0.0004
6	0.0017	0.0265	0.0105	0.0002
7	0.0020	0.0337	0.0110	0.0002
8	0.0118	0.0277	0.0132	0.0003
9	0.0083	0.0257	0.0125	0.0001
10	0.0016	0.0372	0.0121	0.0002

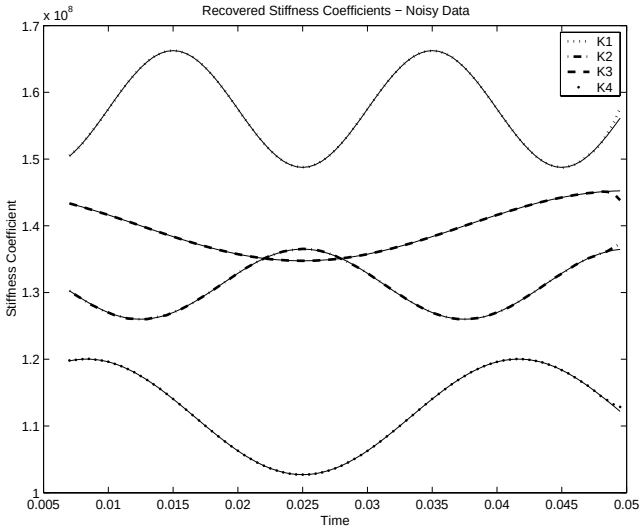

Figure 3: Average of the estimated stiffness coefficients for test function 9 using the Variational Approach (noiseless data).

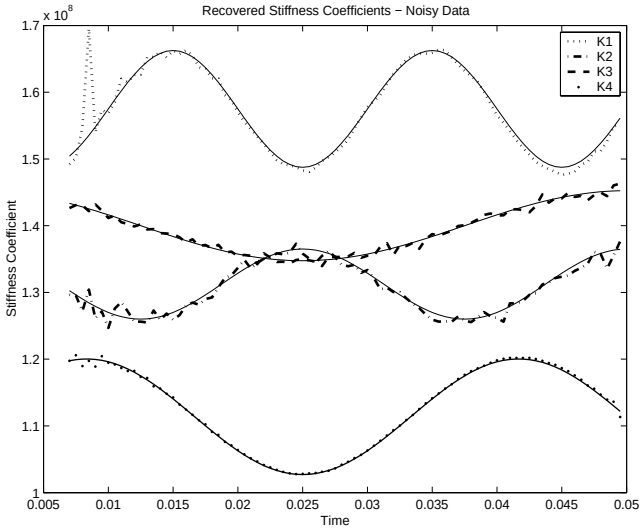

Figure 4: Average of the estimated stiffness coefficients for test function 9 using the Variational Approach (1% of noise).

6.2. ANN Results

In the activation phase the inverse problem is solved by using the weights and bias obtained during the training phase. The robustness of the trained MLP is evaluated employing displacement functions not used in the training phase.

Table 4: Artificial Neural Network results - Individual Average Error for noisy data.

Function Case	$E(\hat{\mathcal{K}}_1)_{mean}$	$E(\hat{\mathcal{K}}_2)_{mean}$	$E(\hat{\mathcal{K}}_3)_{mean}$	$E(\hat{\mathcal{K}}_4)_{mean}$
1	0.0099	0.0535	0.0021	0.0019
2	0.0256	0.0130	0.0020	0.0060
3	0.0070	0.0135	0.0172	0.0018
4	0.0101	0.0553	0.0022	0.0019
5	0.0246	0.0194	0.0012	0.0021
6	0.0093	0.0167	0.0024	0.0066
7	0.0076	0.0160	0.0060	0.0014
8	0.0065	0.0173	0.0036	0.0047
9	0.0089	0.0155	0.0019	0.0014
10	0.0211	0.0406	0.0017	0.0025

Table 5: Artificial neural network - Individual Standard Deviation for noisy data.

Function Case	$E(\hat{\mathcal{K}}_1)_{mean}$	$E(\hat{\mathcal{K}}_2)_{mean}$	$E(\hat{\mathcal{K}}_3)_{mean}$	$E(\hat{\mathcal{K}}_4)_{mean}$
1	0.0009	0.0150	0.0004	0.0003
2	0.0014	0.0034	0.0002	0.0005
3	0.0008	0.0033	0.0012	0.0003
4	0.0010	0.0146	0.0003	0.0004
5	0.0014	0.0054	0.0002	0.0003
6	0.0008	0.0048	0.0003	0.0009
7	0.0008	0.0052	0.0006	0.0003
8	0.0009	0.0063	0.0004	0.0005
9	0.0008	0.0044	0.0003	0.0003
10	0.0008	0.0109	0.0003	0.0004

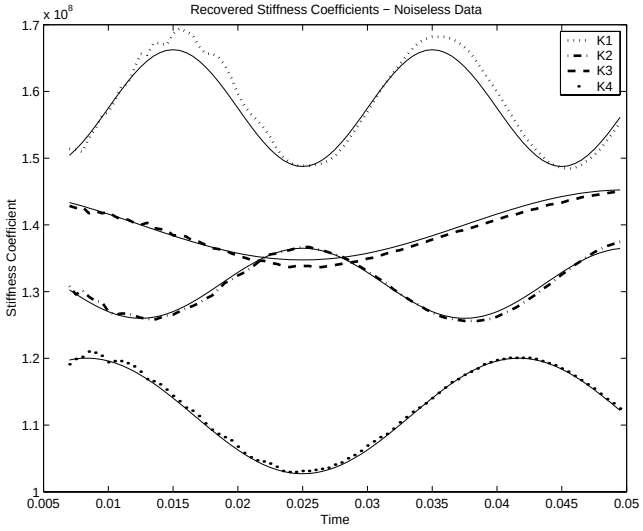

Figure 5: Average of the estimated stiffness coefficients for the test function 9 using the Neural Network technique (noiseless data).

The generalization capacity of the MLP is verified considering 10 different functions defined by eqns. (15) where parameters a_i, b_i and ω_i, for $i = 1, 2, 3, 4$, are presented in Table 1.

Tables 4 and 5 show the average error, defined by eqn. (18), and the standard deviation of the error, defined by eqn. (19), respectively. The estimation using ANN presents small errors ($\mathcal{K} < O(10^{-1})$). Therefore, the use of ANNs is also a good strategy for the estimation of the stiffness coefficient with time dependency. These estimations have a small standard deviation, smaller than those found for the variational method.

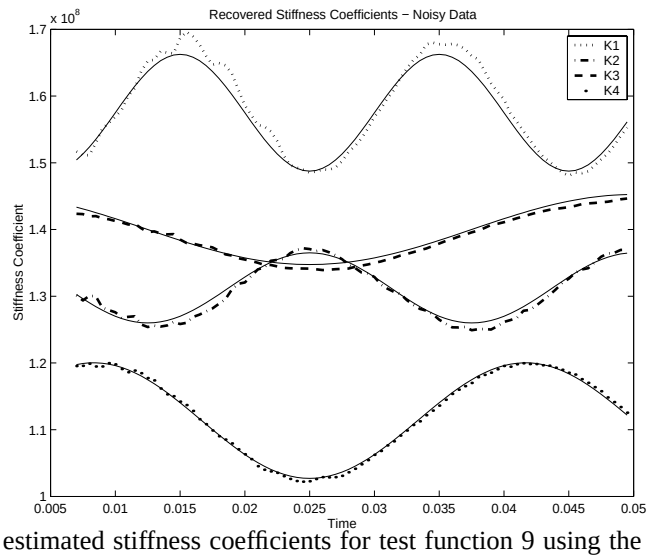

Figure 6: Average of the estimated stiffness coefficients for test function 9 using the Neural Network technique (1% of noise).

Figures 5 and 6 present a qualitative comparison between the estimated stiffness coefficients when noiseless and noisy experimental data are used, respectively, by using the variational approach.

The estimation by ANN of function type-9 is shown in Figures 5 and 6. Some oscillations in the reconstruction is found, even for the noiseless case. However, oscillations present in the estimation considering the noisy case, are smaller than those seen in the inverse solution obtained using the variational approach.

7. CONCLUSIONS

The inverse vibration problem of estimating the unknown stiffness depending on time (damage identification with time dependency) has been addressed using two different approaches, where a simple truss was used as a test example. It should be pointed out that this example is more difficult than a spring-mass system used in a previous work [17]. Several stiffness coefficients are employed to evaluate the methods.

Both strategies showed a good performance, presenting small errors and standard deviations. Table 6 shows the average obtained from the average errors of the 10 test functions studied, previously presented in Tables 2 and 4. For both methods, the highest error is found in the estimation of the $\mathcal{K}_2$ coefficient, whilst the smallest error is found in the estimation of the $\mathcal{K}_4$ coefficient. The estimation using ANN is better for almost all stiffness, only for the stiffness-4 the variational approach presents a small error. Similar behaviour is found related to the standard deviation: the ANN presents smaller standard deviation for $\mathcal{K}_i$ ($i = 1,\ 2,\ 3$), and the variational approach has a smaller standard deviation for $\mathcal{K}_4$.

Table 6: Methodologies Comparison - Individual Average Error for all the test functions (noisy data).

Methodology	$E(\hat{\mathcal{K}_1})_{mean}$	$E(\hat{\mathcal{K}_2})_{mean}$	$E(\hat{\mathcal{K}_3})_{mean}$	$E(\hat{\mathcal{K}_4})_{mean}$
Variational Approach	0.0164	0.1531	0.0513	0.0011
ANN Technique	0.0131	0.0261	0.0040	0.0030

Concerning the computational time requested by the methodologies used in this work, it should be pointed out that the ANN have two different phases: training and activation. The training phase usually is very CPU time consuming, and for the present problem it is requiring some hours. However, this step is done only one time. After the training, the activation phase is very fast, usually takes less than one second. The latter phase represents the real inverse problem solution. Regarding the variational approach, the CPU-time was around few seconds. All computational simulations have been performed in a personal computer with a Pentium IV - 1.6 GHz processor.

Oscillations verified in the inverse solution using an ANN for the noiseless case are also found for all test functions (not shown). However, the error in the reconstruction using an ANN is smaller than those found employing the variational approach for the noisy data.

The mathematical derivation of the equations for the use in the variational approach is the biggest challenge for this methodology. For ANNs, the difficulty lies in the selection of the appropriate data set for training.

The RBF model has also been applied in the estimation of time-dependent stiffness coefficients, however good estimations have not been achieved, denoting that other RBF topologies should be explored in future works.

Acknowledgment
The authors would like to thank the support from FAPESP, CAPES, and CNPq, Brazilian agencies for research support.

REFERENCES

1. O.M. Alifanov, Solution of an inverse problem of heat conduction by iteration methods. *J. Eng. Phys.* (1974) **26**(4), 471-476.

2. M.J. Atalla and D.J. Inman, On model updating using neural networks. *Mechanical Systems and Signal Processing* (1998) **12**(1), 135-161.

3. S.V. Barai and P.C. Pandey, Time-delay neural networks in damage detection of railway bridges. *Adv. Eng. Software* (1997) **28**, 1-10.

4. H.F. de Campos Velho, Inverse problems: Basic concepts and applications, *IV Encontro de Modelagem Computacional (IV Meeting on Computational Modeling)*, Nova Friburgo(RJ), Brazil, 12-14 November, 2001, pp.63-79.

5. D.A. Castello and F.A. Rochinha, On the identification of constitutive parameters of viscoelastic materials by means of a time domain technique, *Proceedings of the 4th International Conference on Inverse Problems in Engineering (ICIPE)*, Angra dos Reis(RJ), Brazil, 26-31 May, 2002, pp. 259-266.

6. L.D. Chiwiacowsky and H.F. de Campos Velho, Different approaches for the solution of a backward heat conduction problem. *Inverse Problems in Engineering* (2003) **11**(6), 471-494.

7. S.W. Doebling, C.R. Farrar, M.B. Prime and D.W. Shevitz, *Damage Identification and Health Monitoring of Structural and Mechanical Systems from Changes in their Vibration Characteristics: A Literature Review*, Los Alamos National Laboratory, report LA-13070-MS, USA, 1996.

8. J. Hadamard, *Lectures on the Cauchy Problem in Linear Partial Differential Equations*, Yale University Press, New Haven, 1923.

9. S. Haykin, *Neural Networks: A Comprehensive Foundation*, Macmillan, Prentice Hall, New York, 1993.

10. C.H. Huang, A non-linear inverse vibration problem of estimating the time-dependent stiffness coefficients by conjugate gradient method. *Int. J. Numer. Meth. Eng.* (2001) **50**, 1545-1558.

11. C.H. Huang, An inverse vibration problem for simultaneously estimating the time-dependent stiffness coefficients, *Proceedings of the 4th International Conference on Inverse Problems in Engineering (ICIPE)*, Angra dos Reis(RJ), Brazil, 26-31 May, 2002, pp. 235-242.

12. Y. Jarny, M.N. Özisik and J.P. Bardon, A general optimization method using adjoint equation for solving multidimensional inverse heat conduction. *Int. J. Heat Mass Transfer* (1991) **34**(11), 2911-2919.

13. R.I. Levin and N.A.J. Lieven, Dynamic finite element model updating using neural networks. *J. Sound Vibr.* (1998) **210**(5), 593-607.

14. M. Nadler and E.P. Smith, *Pattern Recognition Engineering*, John Wiley & Sons, New York, 1993.

15. N.M. Newmark, A method of computation for structural dynamics, *ASCE - J. Eng. Mech. Div.* (1959) **85**, 67-94.

16. W.M. Ostachowicz and M. Krawczuk, Analysis of the effect of a crack on the natural frequencies of a cantilever beam. *J. Sound Vibr.* (1991) **150**(2), 191-201.

17. E.H. Shiguemori, L.D. Chiwiacowsky, H.F. de Campos Velho and J.D.S. da Silva, An inverse vibration problem solved by an artificial neural network. *TEMA: Tendencies on Computational and Applied Mathematics* (2004) – submitted.

18. X. Wu, J. Ghaboussi and J.H. Garrett, Use of neural network in detection of structural damage. *Comput. Struct.* (1992) **42**, 649-659.